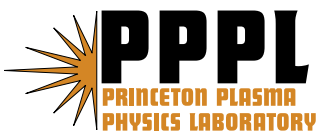# Princeton Plasma Physics Laboratory

Non-inductive Solenoid-less Plasma Current Start-up in NSTX Using Transient CHI

R. Raman, D. Mueller, T.R. Jarboe, B.A. Nelson,
M.G. Bell, M. Ono, T. Bigelow, R. Kaita, B. LeBlanc,
K.C. Lee, R. Maqueda, J. Menard, S. Paul, and L. Roquemore

May 2007

Princeton Plasma Physics Laboratory
Report Disclaimers

Full Legal Disclaimer

Trademark Disclaimer

PPPL Report Availability

Princeton Plasma Physics Laboratory:

http://www.pppl.gov/techreports.cfm

Office of Scientific and Technical Information (OSTI):

http://www.osti.gov/bridge

Related Links:

U.S. Department of Energy

Office of Scientific and Technical Information

Fusion Links

Non-inductive Solenoid-less Plasma Current Start-up in NSTX Using Transient CHI

R. Raman[1], D. Mueller[2] , T.R. Jarboe[1], B.A. Nelson[1], M.G. Bell[2], M. Ono[2], T. Bigelow[3], R. Kaita[2], B. LeBlanc[2], K.C. Lee[4], R. Maqueda[5], J. Menard[2], S. Paul[2], L. Roquemore[2]

[1] University of Washington, Seattle, WA, USA
[2] Princeton Plasma Physics Laboratory, Princeton, NJ, USA
[3] Oak Ridge National Laboratory, Oak Ridge, TN, USA
[4]University of California-Davis, CA, USA
[5] Nova Photonics, Princeton, NJ, USA

ABSTRACT

Coaxial Helicity Injection (CHI) has been successfully used in the National Spherical Torus Experiment (NSTX) for a demonstration of closed flux current generation without the use of the central solenoid. The favorable properties of the Spherical Torus (ST) arise from its very small aspect ratio. However, small aspect ratio devices have very restricted space for a substantial central solenoid. Thus methods for initiating the plasma current without relying on induction from a central solenoid are essential for the viability of the ST concept. CHI is a promising candidate for solenoid-free plasma startup in a ST. The method has now produced closed flux current up to 160 kA verifying the high current capability of this method in a large ST built with conventional tokamak components.

1. INTRODUCTION

The Spherical Torus (ST) is capable of simultaneous operation at high beta and high bootstrap current fraction [1]. These advantages of the ST configuration arise as a result of its small aspect ratio. At the low aspect ratios needed for an ST reactor, elimination of the central solenoid is necessary. Thus current generation methods that do not rely on the central solenoid are

necessary for the viability of the ST concept. Elimination of the central solenoid could also lead to a more compact tokamak [2]. The National Spherical Torus Experiment (NSTX) is exploring the technique known as Coaxial Helicity Injection (CHI) [3] as a method to produce the initial plasma and sufficient toroidal plasma current to allow other methods of non-inductive current drive and sustainment to be applied. The method of CHI has been used in Spheromaks, in other STs [4-8], and in a large aspect ratio tokamak [9].

Helicity injection current drive in a ST was first conducted on the Current Drive Experiment-Upgrade (CDX-U) at the Princeton Plasma Physics Laboratory (PPPL) [10]. For enabling CHI operation, the stainless steel vacuum vessel of NSTX has toroidal ceramic breaks that allow the inner and outer components of the vessel to be electrically separated from each other. The inner vessel components comprising of the center stack and the inner divertor plates act as the cathode while the outer vessel and the outer divertor plates act as the anode. Poloidal field coils located beneath the lower divertor plates are used to produce magnetic field that connect the lower inner and outer divertor plates. During CHI operation an external power supply is used to drive current on these field lines. This current is referred to as the injector current. At sufficiently high levels of the injector current, the minimum value referred to as the bubble burst current magnitude, when the ΔB_{tor}^2, ($J_{pol} \times B_{tor}$) stress across the current layer exceeds the field-line tension of the injector flux, the poloidal field connecting the lower divertor plates (known as the injector flux) stretches in to the vessel [3]. Under appropriate conditions, the field lines near the injector region reconnects, allowing the field lines that have extended into the vessel to form a closed magnetic ring.

CHI can be applied in two ways. In both methods the toroidal plasma current produced by CHI initially flows on open field lines joining the electrodes. In order to produce toroidal plasma current on closed flux surfaces magnetic reconnection must occur. In the first approach referred to as *steady state* or *driven* CHI, closed flux generation relies on the development of some form of non-axisymmetric plasma perturbation. This mode of CHI operation, in which the injector circuit is continuously driven for a time longer than the timescale for resistive decay of the toroidal current ($t_{pulse} > \tau_{L/R}$) was initially studied in the early CHI experiments in NSTX [11]. However, for the purpose of initial plasma startup it was found in the HIT-II ST that a new mode of CHI operation in an ST, referred to as *transient* CHI [12], which involves only axisymmetric magnetic reconnection works very well and produces useful closed flux equilibrium. In transient CHI, the initial poloidal field configuration is chosen such that the plasma carrying the injected current rapidly expands into the chamber. When the injected current is rapidly decreased, magnetic reconnection occurs near the injection electrodes, with the toroidal plasma current forming closed flux surfaces. The method of transient CHI has now been successfully used on NSTX producing an unambiguous demonstration of closed-flux current generation without the use of the central solenoid [13].

2. HARDWARE UPGRADES THAT ENABLED IMPLEMENTATION OF TRANSIENT CHI IN NSTX

NSTX is a 0.85 m major radius, 0.65 m minor radius machine with a vessel volume of 30 m^3. Toroidal ceramic breaks at the top and at the bottom of the stainless steel vessel allow the inner and outer components of the vessel to be electrically biased enabling CHI operation. The lower divertor region where the discharge originates is referred to as the injector region. The upper

4

divertor region is referred to as an absorber because the $E \times B$ flow that arises as a result of voltage application across the inner and outer divertor plates is away from the injector region and into the absorber region.

Several hardware upgrades were necessary to make transient CHI work on NSTX. These include: The installation of a capacitor based injector power supply and improvements to pre-ionization. These are described below.

Power supply upgrades: Initial transient CHI experiments used the DC rectifier power supply designed for use in the driven CHI experiments. At the lower levels of gas injection that are required for transient CHI, gas breakdown became very unreliable. This is because in the absence of sufficient load current, the thyristor switching units in the power supplies could not maintain a constant voltage across the electrodes. In addition, once the discharge initiated, as a result of the significant external inductance required to operate the power supply the injector current could not be rapidly reduced, as required for transient CHI. Experiments on the HIT-II concept exploration device showed that a capacitor based power supply would be more suitable for transient CHI startup [12]. As a result a suitable power supply was designed to meet the requirements for transient CHI operation in NSTX.

The capacitor was sized so as to be able to provide the energy needed for gas breakdown of all the injected gas and heating to meet and exceed the inductive stored energy in the resulting plasma discharge ($\frac{1}{2} L_p I_p^2 < E_{cap} = \frac{1}{2} CV^2$), and capable of providing adequate current to exceed the bubble burst current requirement. The minimum injector current to meet the bubble burst condition is given as $I_{inj} = 2\psi_{inj}^2 /(\mu_o^2 d^2 I_{TF})$, where I_{TF} is the current in the toroidal field coil, d is the width of injector flux "footprint" [3] on the electrodes and ψ_{inj} is the injector poloidal flux

that connects the inner and outer divertor plates. For NSTX, this current varies from a few kA to 30 kA.

Figure 1 is an electrical schematic that shows the power supply components needed for transient CHI operation. A 50 mF capacitor bank, the capacitance of which can be varied from 5 to 50 mF, provides the required injector current. Although the capacitor bank was designed for 2 kV operation, present experiments were restricted to 1.7 kV. The system is comprised of up to ten 5 mF capacitors in parallel and an ignitron switch. A 50 mΩ resistor in series with each capacitor protects the system in case of a short circuit within a capacitor. With all capacitors in parallel, the overall system resistance is about 5 mOhm. This in combination with about 1 µH of external inductance ensures that the capacitor bank system is critically damped. Most of the external inductance is due to five RG-218 coaxial cables connected in parallel, which are used for current transmission from the capacitor bank to the main CHI current feed terminals on NSTX. The peak current capability of this system is about 50 kA, with a current pulse quarter-cycle time of 2 ms. The current pulse width ensures that voltage is applied for a sufficiently long time to meet the required volt.seconds to displace the toroidal flux inside the NSTX vessel as the CHI produced plasma fills the NSTX vessel. This is dependent on the applied injector voltage as this sets the rate at which toroidal flux crosses the injector and absorber gaps: $V_{inj} = d\phi_{tor}/dt$. For nominal NSTX conditions with 0.3 T on axis, there is about 1.4 Wb of toroidal flux inside the vessel. For 1 kV across the injector electrodes, the time needed to displace all of the toroidal flux within the vacuum vessel is about 1.4 ms.

For further protection, for example in case the CHI discharge fails to initiate, the capacitor bank is automatically discharged into a resistive load about 80 ms after the switch ignitron is triggered.

In addition to this a second capacitor discharge resistor is added in parallel to the main capacitors. This is used for rapidly reducing the injector current after the CHI discharge has filled the vessel. Typically, 0.8 ms into a CHI discharge, an ignitron connected in series with this resistor, which has a resistance of 12.5 mOhms, is energized. This causes left over capacitor bank energy to be quickly discharged through this resistor, which causes the injector current to be rapidly quenched.

Improvements to the pre-ionization system: Between 2003 and 2005 as a result of steady improvements to the gas injection system used for injecting the required pre-fill gas needed for the CHI discharge, the total amount of injected gas was reduced from 40 Torr.L in 2003 to 2 Torr.L during 2006. This new level of gas injection is the same as that used as pre-fill for normal inductive operation in NSTX. Typically about 50 eV per ion is needed for ionization and about an additional 60 eV per ion to increase the plasma temperature to 20 eV. In previous experiments (during 2004), the lowest amount of injected gas that could be injected and still achieve reliable breakdown was too high to achieve a reasonable temperature. To overcome this limitation, the gas injection for CHI was changed from four ports in the lower inner divertor plate to a single port in a small ($\sim 100\ l$) cavity below the toroidal gap between the lower divertor plates. In addition 10 kW of 18 GHz microwave power was injected into the cavity to pre-ionize the gas. These changes allowed breakdown to be achieved with much less total gas injected than previously possible, and at a level comparable to the amount of gas normally used for inductive plasma startup. The energy needed for ionizing and heating the injected gas was thereby reduced to a few kJ, considerably less than that available from the capacitor bank. Figure 2 shows the initiation of a weak plasma in the lower divertor gap. This is caused by microwave pre-ionization of the gas injected below the lower divertor plates that emerges from the divertor gap region, and

occurs without any voltage application to the divertor plates. During this time, when a voltage is also applied from the charged capacitor bank, easier conduction across the divertor gap as a result of the presence of this ionized gas immediately causes full breakdown of the injected gas, which is subsequently followed by the capacitor bank discharge.

As a result of these improvements to the pre-ionization system, the breakdown of the injected gas was synchronized to about a milli-second of the voltage application time. This in combination with the small amount of injected gas in the injector region meant that considerably less gas was present in the absorber region at the time voltage was applied to the electrodes. As a result, absorber arcs, which were problematic during the long pulse driven CHI discharges became benign during the transient CHI discharges. The absorber arc is a condition when part of the injected current bridges the upper divertor insulator and flows along the vessel structure. In transient CHI discharges, although absorber arcs occur, they do not terminate the CHI discharge as they did during the long pulse discharges. This is because the impedance of the absorber arc, because there is now much less gas in the absorber region, is comparable to that of the main plasma load. During the steady-state experiments, for which considerably more gas injection was necessary, the impedance of an absorber arc was considerably less than that of the CHI plasma discharge, which caused the CHI discharge to immediately quench soon after the initiation of an absorber arc.

3. EXPERIMENTAL RESULTS FROM TRANSIENT CHI OPERATION IN NSTX

CHI discharges are initiated by first energizing the toroidal field coil and the poloidal field coils to produce the injector flux. A preprogrammed amount of deuterium gas is then injected into the

region below the lower divertor plates. About two ms before the application of voltage from the CHI power supply, microwave power is injected into the lower divertor region. After the capacitor bank is discharged, and as the injector current increases and exceeds the bubble burst threshold, the poloidal field connecting the lower divertor gap expands to fill the vessel. After a programmed delay of 3 – 5 ms, when the plasma has expanded into the chamber and the toroidal plasma current is near its peak value, the capacitor bank is short-circuited by a "shorting" ignitron that discharges remaining capacitor bank energy through a discharge resistor, causing the injector current to decay rapidly. The plasma column detaches from the injector region to form closed flux, analogous to the detachment of a solar flare on the surface of the sun. A feature of CHI plasma generation using this method is that flux closure can be demonstrated unambiguously by the persistence of plasma current after the injector current has been reduced to zero. During these experiments, the NSTX central solenoid was disconnected from its power supply.

In Figure 3, we show traces for the injector current, the plasma current and voltage across the capacitor bank for a discharge without the presence of an absorber arc. The capacitor bank is discharged at 5 ms. This causes a capacitor based voltage snubber, which is connected across the injector region, to charge up resulting in the initial transient in the injector current, which increases to 2.4 kA. Plasma breakdown occurs shortly after 6 ms, which causes the injector current to increase from 1.2 to 1.5 kA. At 8 ms, the capacitor shorting ignitron is energized, which causes the left over capacitor bank energy to discharge, causing the more rapid droop in the capacitor bank voltage. This can be seen in the capacitor bank voltage trace, which now shows a more rapid drop in voltage. Simultaneously, the injector current also shows a more rapid decrease. At about 10-11 ms, the capacitor bank current has essentially reduced to zero, which

means that the CHI power system is off and the CHI plasma load is no longer being actively driven by an external power supply. Therefore, the left over persisting plasma current can only result from a decaying closed flux current equilibrium. Calculations that take into consideration the charge transfer from the capacitor bank show that for this discharge only about 8 kJ of capacitor bank energy was expended to generate about 60 kA of closed flux current. Note that the obtained toroidal current is amplified many times over the injector current. On NSTX, the highest value of this current multiplication factor is 70, compared to about 6 on the HIT-II experiment. The fast visible camera images show the growth of the CHI discharge. At 7.2 ms one can see the discharge extending from the injector region. At 8 and 8.4 ms, it has fully extended into the vessel. Starting from 9 ms, it begins to shrink in elongation and at 11 ms it is disconnected from both the injector and the absorber region. It is useful to note that in this discharge an absorber arc was not generated.

Figure 4 shows two discharges during which an absorber arc was generated. For discharge 120888, the absorber arc initiates shortly after 6 ms, which causes the magnitude of the injector current to rapidly increase from about 2-3 kA (prior to the arc) to 25 kA at the time of peak arc intensity. The absorber arc can be seen from the bright light emission in the form of a ring that develops in the 6.17 and 8.1 ms camera images. The large amount of absorber arc current resulted from the use of a larger capacitor bank at higher voltage. The discharge in Figure 3 used 3 capacitors charged to 1.5 kV, whereas the discharge in Figure 4 used 9 capacitors at 1.7 kV. The discharge shown in Figure 4 was operated at higher values of the toroidal field and injector flux, which requires the application of a higher voltage. It resulted in about 160 kA of persisting closed flux current after the injector current is reduced to zero. Present Metal Oxide Varistors (MOV) used for voltage snubbing begin to significantly conduct starting at 1.7 kV. Thus in order

to maintain the higher voltage for an adequate amount of time more capacitors were used. However, since only a small amount of this energy is needed for the resulting CHI discharge, as shown by the result in Figure 3, the remaining unused capacitor bank energy is transformed into a high current absorber arc.

The discharge shown in Figure 3 has a longer current decay than the one shown in Figure 4, even though it has a lower amount of closed flux current at the time the injector current is reduced to zero, because this discharge has no absorber arcing. Absorber arcing is a condition when an undesirable current path along the upper insulator surface could potentially cause surface insulator materials to enter the plasma, making it more resistive. By operating the discharges shown in Figure 4, with lower number of capacitors, the extent of absorber arcing could be considerably reduced or eliminated, which should increase the current decay time in these discharges. Future experiments in NSTX will optimize this scenario by reducing the extent of MOV conduction current, which should allow one to operate these discharges with fewer capacitors and at higher voltage, which should help to considerably reduce the extent of absorber arc current.

As shown in Figure 4 for a lower current discharge, for which Thomson scattering [14] data was available, the results show the electron temperature to be in the 10 to 20 eV range, and the electron density to be below 5×10^{18} m^{-3} in the bulk of the plasma cross-section. The data also shows that the profile at 10 ms is less hollow compared to that at 8 ms. This observation is consistent with the method of CHI current generation, which initially drives current in the edge. After the generation of closed flux as the profile relaxes, one expects the current to penetrate to the interior, which should result in the profiles becoming less hollow, as indicated by the electron temperature profiles. Taking the measured electron temperatures of about 15 – 20 eV and

assuming Spitzer resistivity, and a typical plasma inductance of about 0.5 - 1 µH, results in a current-decay e-folding time on the order of 5 ms, which is consistent with the observation that the current persists for about 10 ms after the injector current has been reduced to zero.

In Figures 5 and 6 we show equilibrium reconstructions for discharges with very long current persistence. In the discharge shown in Figure 5, a 30 kA discharge is maintained for about 100 ms, thereafter it reduces to about 20 kA and is maintained at this level until 400 ms, at which time the current in the vertical field coils is reduced to zero. For the discharge shown in Figure 6, a higher initial current of about 40 kA gradually decays over the same 400 ms interval. For the first 20 ms, these discharges are similar to the usual transient CHI discharges such as the ones shown in Figures 3 and 4, and during the phase after the injector current is reduced to zero equilibrium reconstructions are consistent with the presence of closed flux surfaces. The experimentally measured poloidal magnetic field at 40 sensors and poloidal flux at 44 flux loops distributed poloidally, are used in the computation of the Grad-Shafranov plasma equilibrium. The LRDFIT Grad-Shafranov equilibrium code [15] was used for these reconstructions. The code uses a circuit equation model of the plasma, vessel, and passive plate currents to constrain the equilibrium fits. Electron temperature and electron density for these discharges were not available. The camera images are very faint and difficult to resolve, however, at times, a definable image is seen, for example as seen for the discharge in Figure 6. In many of the long duration persisting plasmas, similar to the one shown in Figure 5, a 20 kA current persists at a constant current level for as long as the vertical field is maintained. The plasma current decreases when the vertical field is reduced, suggesting that during the extended phase (beyond 20 ms) a collisionless electron current channel is maintained in the region indicated by the camera images and equilibrium reconstructions because of favorable particle drifts. The discharge shown in

Figure 6 is unusual in this regard as initially about 40 kA of toroidal current is present that over a period of 400 ms gradually decays in magnitude, suggesting that collisions may be contributing to a reduction in current. Indeed the interferometer diagnostic shows a line averaged electron density to be in the range of 1-2 x 10^{12} cm^{-3}, throughout the 400 ms discharge duration. The assumed interferometer path length is 67 cm, which represents the minor cross-section of the NSTX vessel. However, because this CHI plasma occupies a much smaller fraction of the NSTX cross-section the actual electron density is expected to be higher than that indicated by the interferometer diagnostic. Local measurements of the electron density and temperature for these decaying plasmas will be attempted in future using the Thomson scattering diagnostic. Starting from 400 ms the vertical field is reduced to zero, which causes the faster decay in plasma. This is the first observation of such long persisting plasmas produced using CHI at this level of toroidal current that show current decay over time.

Discharges of the type shown in Figures 5 and 6 are produced when the wall pumping increases. With increased wall pumping, one finds that during the decay phase of a CHI discharge the electron density drops to low levels, to below the measurement capability of the Thomson Scattering diagnostic leading to a current channel that persists for as long as the vertical field is maintained, probably because the decaying plasma becomes collisionless. A good example of such a discharge is the one shown in Figure 5. Thus for example, if one were to start with a discharge shown in Figure 4 and increased the wall pumping (for example as a result of a long He conditioning discharge), the discharge would end up with a long persisting plasma. The discharge in Figure 6 is unusual as it has similar vertical field programming as that for the discharge shown in Figure 5, however it shows the current to decay over a long time. The probable cause is that this discharge is not collisionless, and so must have higher electron density

than the discharge in Figure 5. In general, discharges such as those shown in Figures 5 and 6 are very sensitive to wall conditions. While discharges such as the one shown in Figure 5 are frequently produced, the discharge in Figure 6 is more difficult to produce, probably because the wall pumping requirements cover a very narrow range. With too much wall pumping a discharge such as the one in Figure 5 is produced and too little wall pumping produces a discharge such as the one shown in Figure 4.

The maximum plasma current is given by the relation $I_p = I_{inj}(\psi_{Toroidal}/\psi_{inj})$ [3]. As one increases the ratio of the toroidal flux to injector flux, the current multiplication ratio increases. As one increases the injector flux more poloidal flux is injected, however, from the bubble burst relation described in section 2, more injector current is also needed. The maximum allowable injector current would eventually be determined by the allowable current limits on the electrode surface, which is dictated by the choice of the electrode material. If the plasma is too resistive, for example as a result of a large absorber arc current, or too much injector current, it would decay at a faster rate and there would be less closed flux current remaining at zero injector current. These optimizations to maximize the plasma current have not been adequately performed in the NSTX transient CHI experiments so far. The discharges in Figure 4 were operated at higher values of the toroidal field, 0.5 T on axis for shot 120842 and 0.52 T on axis for shot 120888, compared to 0.4 T for the discharge shown in Figure 3. The discharges in Figures 5 and 6 both have about 80 to 90 kA of closed flux current at the time the injector current is reduced to zero, although this is not clearly seen in the figure because of the long duration time axis. These were also operated at 0.5 T on axis. Future experiments in NSTX will do a more complete optimization of the three parameters (injector current, toroidal flux and injector flux) to maximize the achievable closed flux current at zero injector current.

Scaling to larger machines: Transient CHI experiments conducted on NSTX have considerably benefited from previous work on the much smaller HIT-II machine. HIT-II was a concept exploration device. An important difference between the NSTX and HIT-II results is that the injector current on NSTX, in the absence of absorber arcing, is typically a few kA, whereas on HIT-II it is typically 15 – 30 kA. The current multiplication ratio of the plasma current to injector current on HIT-II is 6 - 7, whereas NSTX has achieved a current multiplication ratio up to 70. This favorable scaling of CHI with increasing machine size, summarized in Table 1, occurs because the current multiplication factor, which is obtained from the condition for helicity injection threshold, given as $I_p = I_{inj}(\psi_{Toroidal} / \psi_{inj})$ increases in proportion to the toroidal flux [3,15]. However, Table 1 also shows the theoretical maximum for the current multiplication to be about twice that achieved by both machines.

In larger machines, as the field line length increases, because of an increase in injector impedance higher voltages may be necessary. However, other factors such as improved pre-ionization and additional heating such as from high power radio frequency heating, could be used to increase the plasma conductivity and reduce the voltage requirements. For a given input power, reducing the electron density should allow the electron temperature to increase and cause the plasma resistivity to decrease. Present observation is that the NSTX device, which is much larger than HIT-II routinely operates at lower voltages of ~1.7 kV compared to 2.5-4 kV in HIT-II. However, further experimental results are needed from NSTX to clearly assess the voltage requirements for larger machines.

The implications of these scaling results are quite favorable for a larger ST, such as a CTF [16] which has a major radius R = 1.2 m, maximum toroidal field on axis B_T = 2.5 T and a toroidal flux $\psi_T \sim$ 15 Wb. For similar values of the injector current as on HIT-II and current multiplication factors as on NSTX, CHI produced toroidal plasma currents much in excess of 1 MA are not unrealistic in CTF sized machines. At this level of current, other well-established non-inductive current drive methods, such as neutral beam injection and radio frequency current drive, could ramp the current to the required levels.

4. CONCLUSIONS

Using the method of transient CHI, NSTX has produced about 160 kA of closed flux toroidal current for an unambiguous demonstration of closed flux current generation by CHI in a large toroidal device. In this method a plasma current is rapidly produced by discharging a capacitor bank between coaxial electrodes in the presence of toroidal and poloidal magnetic fields. The initial poloidal field configuration is chosen such that the plasma rapidly expands into the chamber. When the injected current is rapidly decreased, magnetic reconnection occurs near the injection electrodes, with the toroidal plasma current forming closed flux surfaces. Electron temperatures up to 20 eV have been measured in the plasma, similar to the levels seen on the HIT-II experiment. As time progresses, the measured profiles become less hollow, consistent with the expectations of CHI startup. Some discharges persist for very long durations, and seem to be limited only by the programmed decay in the vertical field. The significance of these results are (a) demonstration of the process in a vessel volume thirty times larger than HIT-II on a size scale more comparable to a reactor, (b) a remarkable multiplication factor of 60 between the

injected current and the achieved toroidal current, compared to six in previous experiments, and (c) for the first time, fast time-scale visible imaging of the entire process that shows discharge formation, disconnection from the injector and the reconnection of magnetic field lines to form closed flux. These significant results indicate favorable scaling with machine size. Future plans are to further increase the plasma current and to couple the CHI produced plasma to induction from the central solenoid. This would be followed by the application of up to 200 kW of microwave power to increase the electron temperature for coupling to other non inductive current drive methods.

ACKNOWLEDGMENTS

17

Figure captions:

Figure 1: Schematic of the CHI power supply circuit showing the location of the voltage snubbing devices (the capacitor based snubber and the Metal Oxide Varistors) in relation to the main capacitor bank, the capacitor shorting resistor and the CHI plasma load. The path of the Absorber arc current is also shown.

Figure 2: Shown are a three dimensional view of the NSTX machine, a line drawing poloidal cross-section of the machine and fast camera visible image of a discharge in which Electron Cyclotron Heating preionization produced a plasma in the lower divertor region. The location of the NSTX center stack in the fast camera image is shown by the vertical red line. The middle figure also shows the polarity of the magnetic fields and vessel voltage. The location of the Absorber and Injector regions is also shown.

Figure 3. A 60 kA CHI discharge that does not produce an absorber arc. Shown are traces for the injector current, the plasma current, the capacitor bank voltage and visible fish eye images from a fast camera diagnostic. The images show evolution of the plasma discharge from the injector region, which fills the vessel, and subsequently shrinks in size.

Figure 4. A discharge (120888) in which about 160 kA of persisting closed flux current is present after the injector current is reduced to zero. A lower current discharge (120842) is also shown along with electron temperature and electron density profiles at 8 and 10 ms. Shown are the injector current, the plasma current, Thomson scattering data (for 120842) and fast camera images for discharge 120888, which show the development of an absorber arc at 6.17 ms. The Absorber arc is seen by the bright visible ring that is seen in the absorber region. The arc can be

seen intensifying at 8.1 ms. For comparison, note that the images from Figure 3 do not show evidence for such a visible light emission in the upper divertor gap.

Figure 5. A long pulse discharge for which equilibrium reconstructions was possible long after the injector current is reduced to zero. Shown are the injector current, the plasma current, the capacitor bank voltage and equilibrium reconstructions at 10 ms, 25 ms, 40 ms and at 100 ms. Most of the increase in the injector current after 6 ms is due to the generation of an absorber arc. An inflection in the capacitor bank voltage can also be seen at this time. Many discharges that show very long current persistence (beyond 20 ms) are similar to this.

Figure 6. A long pulse discharge and equilibrium reconstructions during the long pulse current decay phase. In addition to the traces for the plasma current and the injector current, shown also are fast camera visible images at 32 to 39 ms and equilibrium reconstructions at 15 ms, 30 ms, 100 ms, 200 ms and at 300 ms. This discharge differs from the discharge shown in Figure 5 by having a higher initial current and showing current decay during the long 400 ms phase.

Table 1: Table showing the achieved current multiplication factors in the concept exploration HIT-II device, in NSTX and projected current for a CTF sized device.

19

REFERENCES

[1] M. Ono, S.M. Kaye, Y-K. M. Peng, *et al.,* Nucl. Fusion **40**, 3Y 557 (2000)

[2] F. Najmabadi and the ARIES Team, Fusion Eng. Design, **41**, 365 (1998)

[3] T.R. Jarboe, Fusion Technol. **15**, 7 (1989)

[4] C.W. Barnes, J.C. Fernandez, I. Henins, *et al.,* Phys. Fluids **29**, 3415 (1986)

[5] H.S. McLean, S. Woodruff, E.B. Hooper, *et al.,* Phys. Rev. Lett. **88**, 125004 (2002)

[6] B.A. Nelson, T.R. Jarboe, A.K. Martin, *et al.,* Phys. Plasmas **2**, 2337 (1995)

[7] M. Nagata, T. Kanki, N. Fukumoto, and T. Uyama, Phys. Plasmas **10**, 2932 (2003)

[8] P.K. Browning, G. Cunningham, S.J. Gee, *et al.,* Phys. Rev. Lett. **68**, 1722 (1992)

[9] M.J. Schaffer, private communication (2000)

[10] M. Ono, G.J. Greene, D. Darrow, *et al.,* Phys. Rev. Lett. **44**, 393 (1980)

[11] R. Raman, T.R. Jarboe, D. Mueller *et al.,* Nucl. Fusion **41**, 1081 (2001)

[12] R. Raman, T.R. Jarboe, B.A. Nelson, *et al.,* Phys Rev. Lett. **90,** 075005 (2003)

[13] R. Raman, B.A. Nelson, M.G. Bell, *et al.,* Phys. Rev. Lett. **97**, 175002 (2006)

[14] B. LeBlanc, Rev. Sci. Instrum. **74**, 1659 (2003)

[15] J. Menard, private communication (2006)

[16] X.Z. Tang and A.H. Boozer, Phys. Plasmas **12**, 042113 (2005)

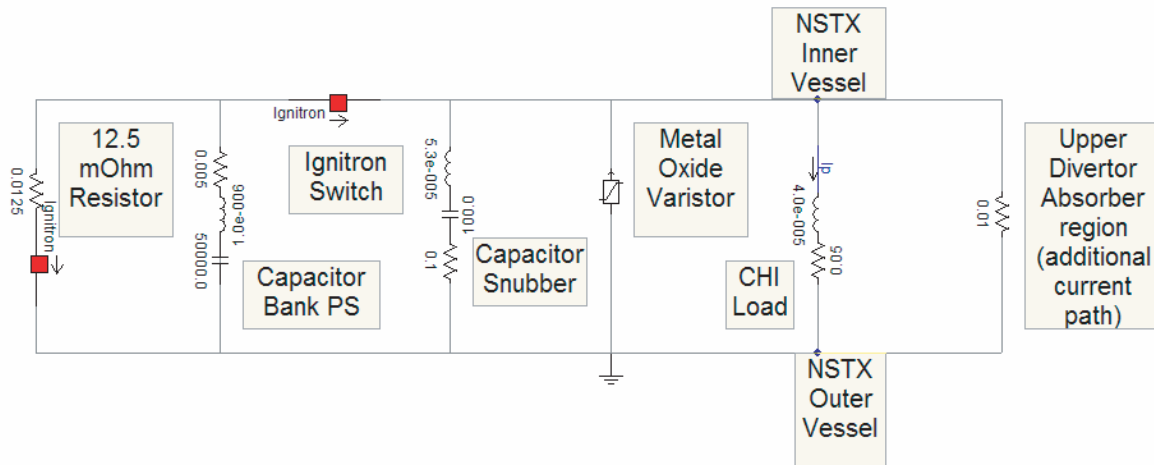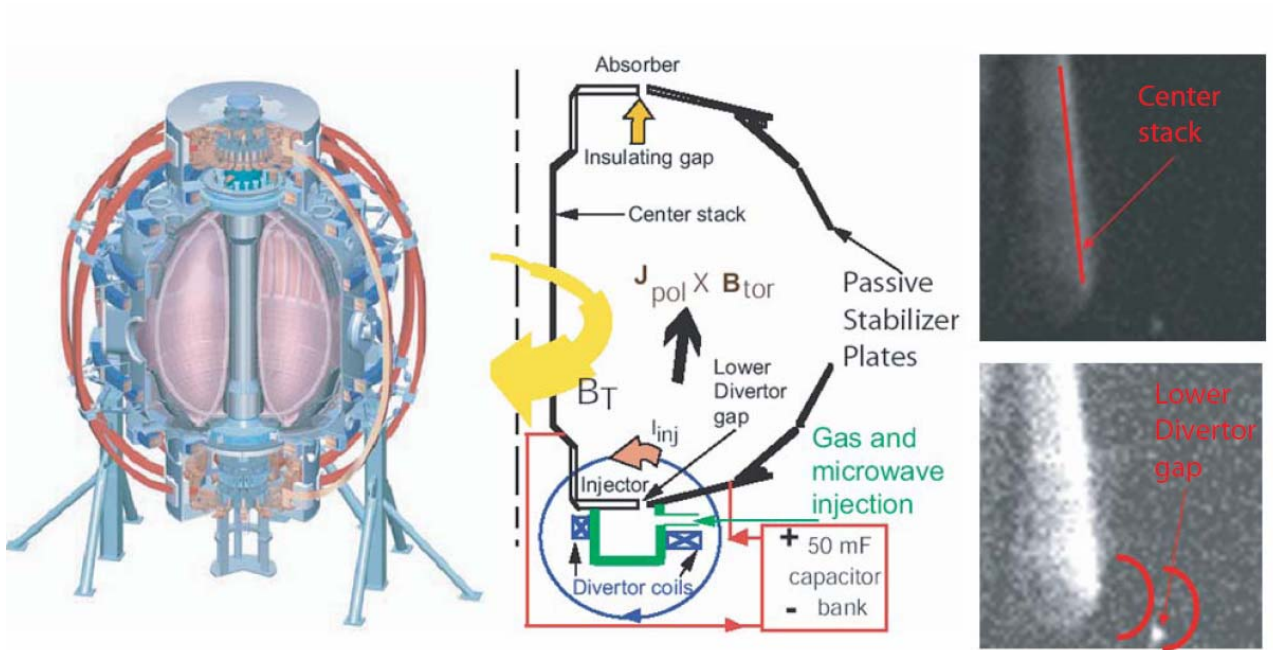[17] M. Peng, Plasma Phys. Control. Fusion **47**, B263 (2005)
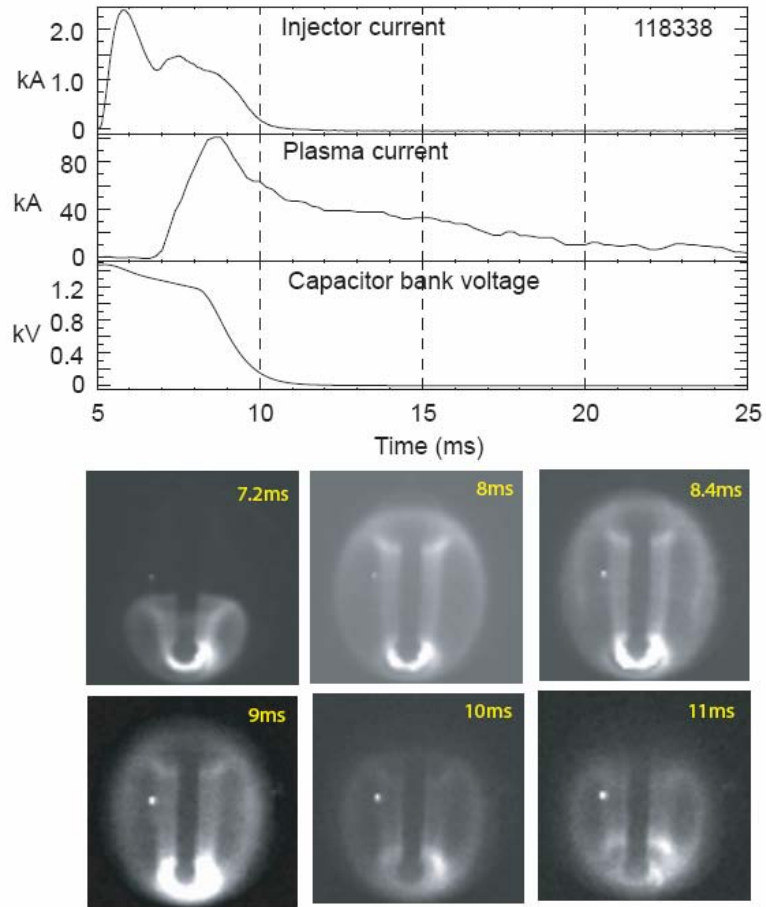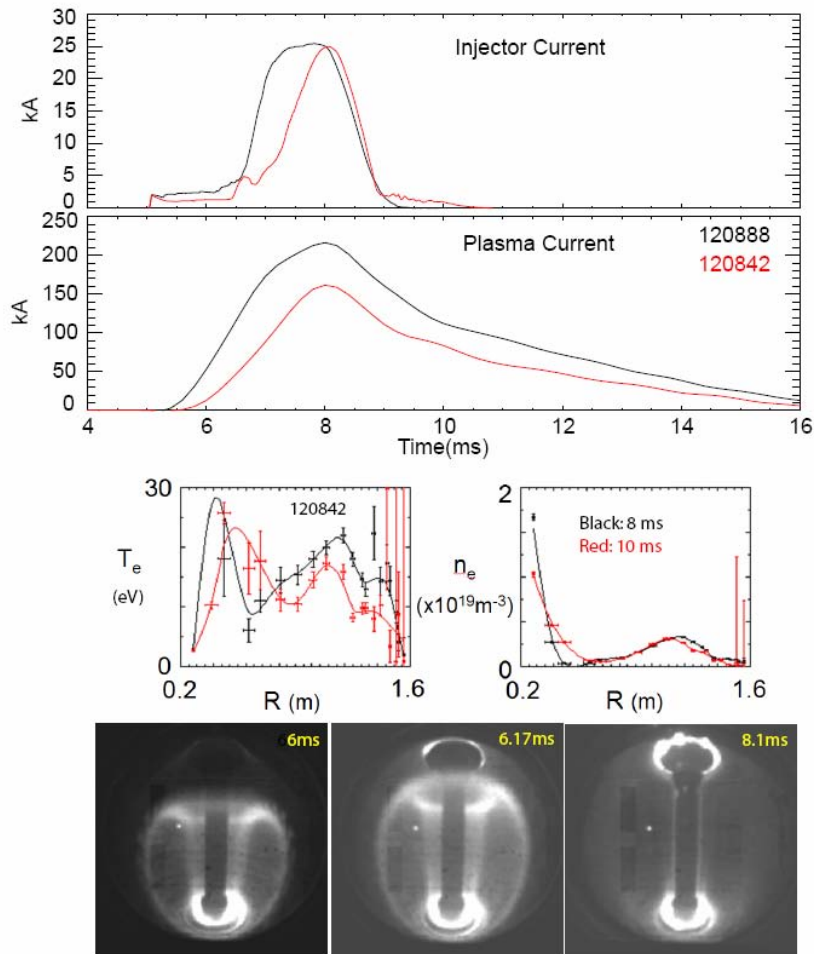
Figure 1

21

Figure 2

Figure 3

23

Figure 4

24
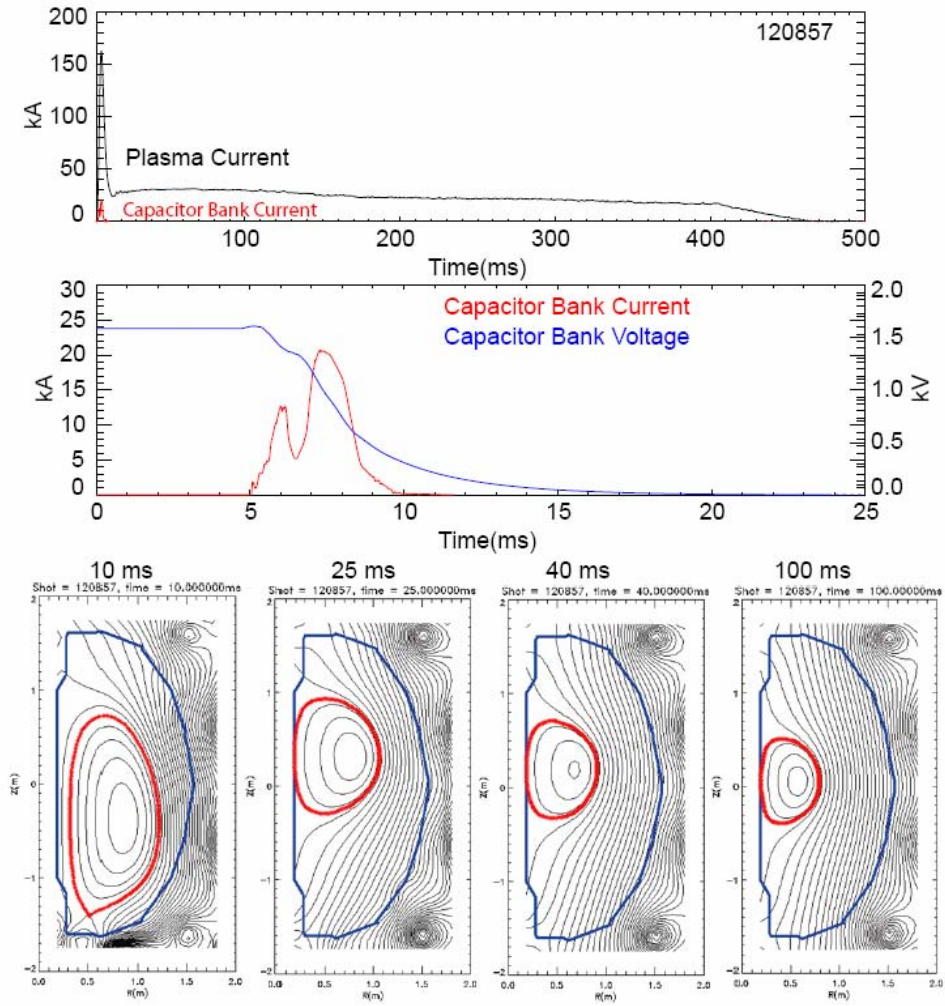
Figure 5

Figure 6
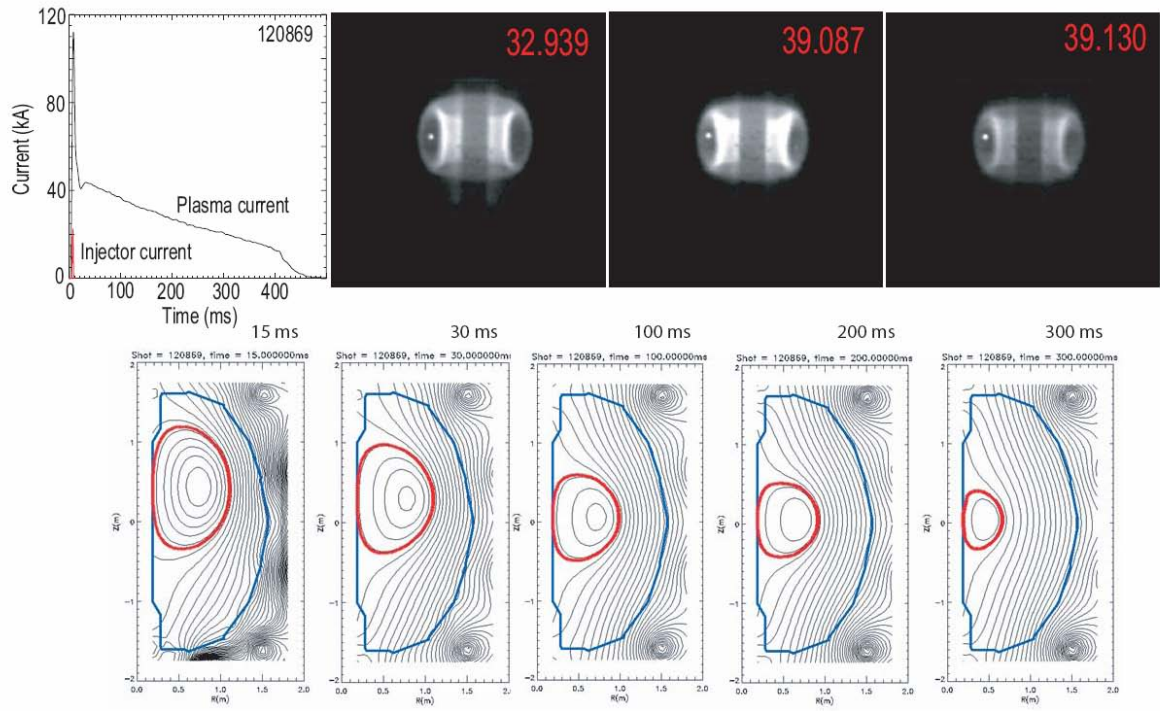
Table 1

Parameter	HIT-II	NSTX	CTF
R(m)	0.3	0.86	1.2
a(m)	0.2	0.68	0.8
Vol(m^3)	0.36	11.2	~38
B_T(T)	0.43	0.41	2.5
k(elongation)	1.5	2.3	3.0
ψ_T (Wb)	0.13	1.30	10-15
ψ_{inj} (mWb)	8	10	>50
I_p/I_{inj} (Meas)	6	70	NA
I_p/I_{inj} (Calc)	16	130	>100
I_{inj}(kA)	15-30	2	2-30
I_p(MA)	0.1	>0.15	>1
L_p(μH)	~0.5	~0.5	<0.5
$E_{indctive}$(kJ)	2.5	>6	~250

The Princeton Plasma Physics Laboratory is operated
by Princeton University under contract
with the U.S. Department of Energy.

Information Services
Princeton Plasma Physics Laboratory
P.O. Box 451
Princeton, NJ 08543

Phone: 609-243-2750
Fax: 609-243-2751
e-mail: pppl_info@pppl.gov
Internet Address: http://www.pppl.gov